ELECTRONIC SUPPORTING INFORMATION

(ESI)

$(TeCl_4)_4(TiCl_4)$ with Isolated Te_4Cl_{16} and $TiCl_4$ Molecules and Second-Harmonic-Generation

Maxime A. Bonnin[†], Klaus Beier[†], Lkhamsuren Bayarjargal[‡], Björn Winkler[‡]*, and Claus Feldmann[†]*

[†]Institute for Inorganic Chemistry (IAC), Karlsruhe Institute of Technology (KIT), Engesserstraße 15, D-76131 Karlsruhe (Germany), E-mail: claus.feldmann@kit.edu

[‡]Institute of Geosciences, Goethe University Frankfurt, Altenhoeferallee 1, D-60438 Frankfurt a. M. (Germany), E-mail: b.winkler@kristall.uni-frankfurt.de

Content

1. Analytical Techniques

X-ray powder diffraction (XRD). X-ray powder diffraction analysis (XRD) of $(TeCl_4)_4(TiCl_4)$ was performed on a Stoe Stadi-P diffractometer (Stoe, Germany) using Cu–$K_{\alpha 1}$ radiation ($\lambda = 154.06$ pm) with a Ge-monochromator. Rietveld refinements were performed with the program TOPAS-Academic (Version 5), using the *cif*-data to confirm the phase purity of the title compound. The refinement was carried out by a simple axial model.

Fourier-transform infrared (FT-IR) spectra of $(TeCl_4)_4(TiCl_4)$ was recorded on a Bruker Vertex 70 FT-IR spectrometer (Bruker, Germany). The samples were measured in reflection with a Platinum A 225 ATR unit.

Thermogravimetry (TG) of $(TeCl_4)_4(TiCl_4)$ was carried out on a Netzsch STA 449 F3 Jupiter device (Netzsch, Germany), using α-Al_2O_3 as a crucible material and reference. Buoyancy effects were corrected by baseline subtraction based on a blank measurement. The samples were measured under dried nitrogen up to 1200 °C with a heating rate of 5 K/min. The Netzsch software PROTEUS Thermal Analysis (Version 5.2.1) was used for graphical illustration.

2. Material Characterization

The crystallographic data and refinement details of $(TeCl_4)_4(TiCl_4)$ are listed in Table S1. The data of the Rietveld refinement are summarized in Table S2. The unit cell of $(TeCl_4)_4(TiCl_4)$ is shown in Figure S1.

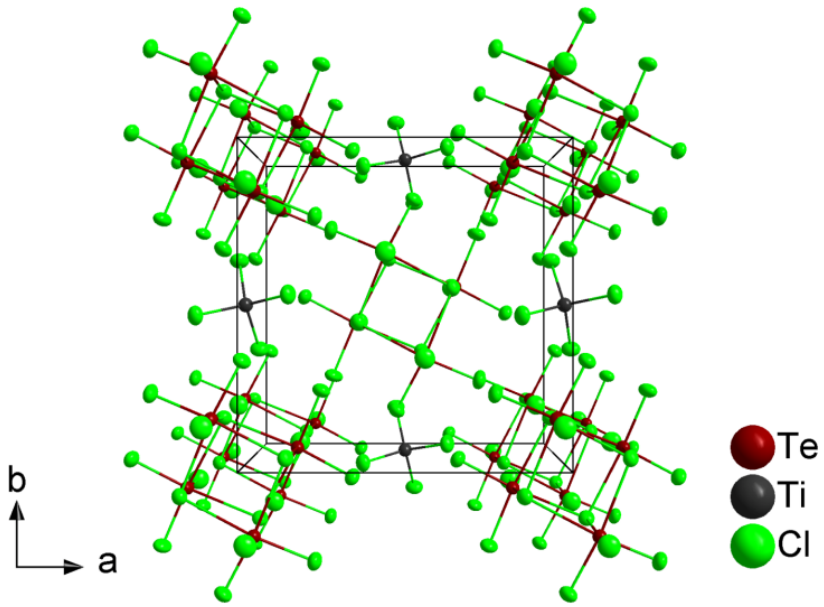

Figure S1. Unit cell of $(TeCl_4)_4(TiCl_4)$.

Table S1. Crystallographic data and refinement details of $(TeCl_4)_4(TiCl_4)$ (recorded at 210 K).

Compound	**$(TeCl_4)_4(TiCl_4)$**
W ($g \cdot mol^{-1}$)	1267.30
Space group	$I\bar{4}$
Flack parameter	0.50(4)
a (pm)	1210.4(2)
c (pm)	1015.2(2)
V (10^6 pm^3)	1487.2(4)
Z	2
$\rho_{calc.}$ ($g \cdot cm^{-3}$)	2.83
μ (mm^{-1})	5.93
λ(Mo–K_α) (pm)	71.073
T (K)	210
Observed reflections	3863
Independent reflections	1960
R_1 ($I \geq 2\sigma_I$)	0.0191
R_1 (all data)	0.0211
wR_2 ($I \geq 2\sigma_I$)	0.0435
wR_2 (all data)	0.0438
GooF	0.997

Table S2. Rietveld refinement details of $(TeCl_4)_4(TiCl_4)$ (recorded at 20 °C)

Compound	**$(TeCl_4)_4(TiCl_4)$**
a (pm)	1222.2
c (pm)	1013.8
R_{wp}	0.0183

In regard of the body-centred cubic (*bcc*) packing of $(TeCl_4)_4$ with $TiCl_4$ in half of the tetrahedral voids (Figure S2), it must be noticed that these tetrahedral voids are distorted as not all edges have the same length.[S1] Compressing a single axis to a tetragonal lattice changes the distortion so that all edges of the tetrahedra become identical (995.1(1) pm). The distortion is related to angles of 98.6(1)° being much smaller than the tetrahedral angle (109.5°). The distance between the center of the $TiCl_4$ tetrahedra and the tetrahedral corners is 656.2(1) pm.

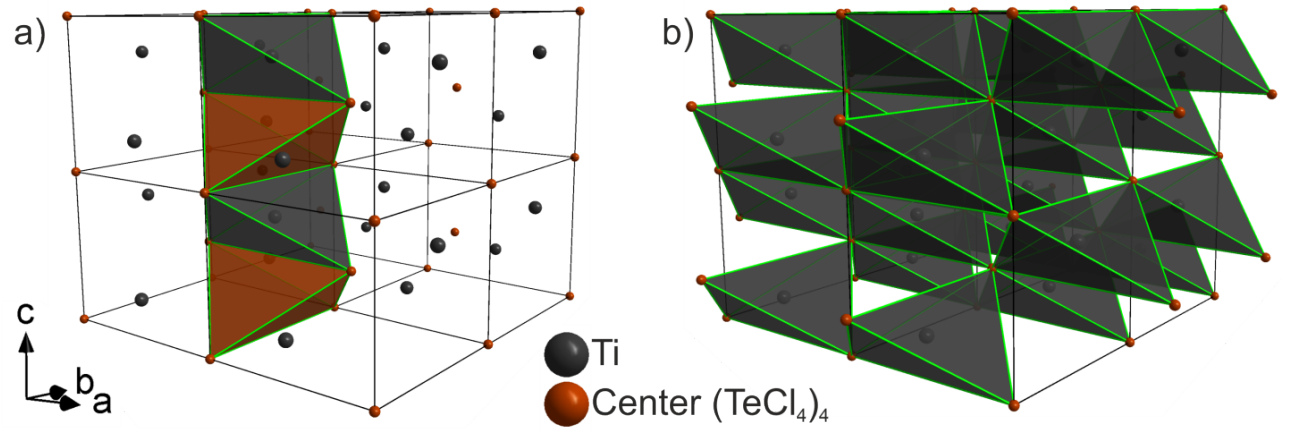

Figure S2. Reduced building units of $(TeCl_4)_4(TiCl_4)$ in a (2×2×2) supercell showing (a) selected and (b) all occupied tetrahedral voids.

The purity of $(TeCl_4)_4(TiCl_4)$ was confirmed by X-ray powder diffraction with Rietveld refinement (*see main paper: Figure 2*), Fourier-transform infrared (FT-IR) spectroscopy (*see main paper: Figure 4a*) and thermogravimetry (TG, Figure S3a) and differential thermal analysis (DTA, Figure S3b). Thermally, the title compound shows three-step decomposition with the first step at 100-150 °C with 14 % mass loss, the second step at 200-400 °C with a mass loss of 82 %, and the third step beginning at 700 °C with a mass loss of 4 %. These mass losses can be attributed to the sublimation of $TiCl_4$ (calculated: 15 %) and the sublimation of $TeCl_4$ (calculated: 85 %). The third minor mass loss of 4 % can be ascribed to the sublimation of elemental tellurium as an impurity, which was already indicated by XRD (*see main paper: Figure 2*).

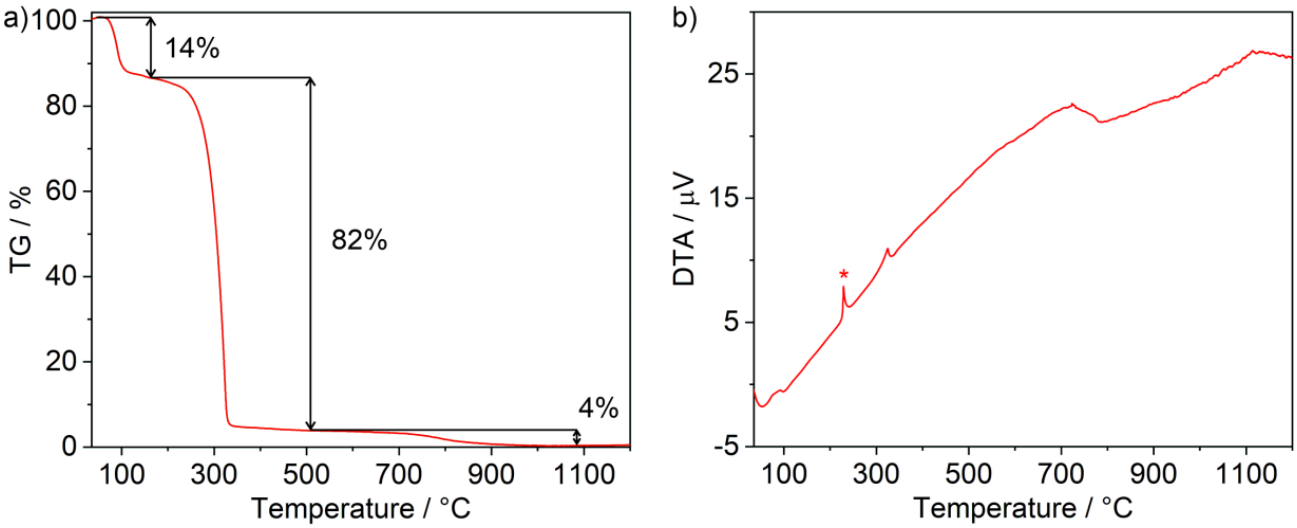

Figure S3. Thermal properties of $(TeCl_4)_4(TiCl_4)$: a) TG and b) DTA (*melting point of $TeCl_4$).

3. Calculations

Atomistic model calculations were carried out within the framework of DFT[S2] and the pseudopotential method using the CASTEP simulation package.[S3] Norm-conserving pseudopotentials were generated "on the fly" using the parameters provided with the CASTEP distribution. These pseudopotentials have been extensively tested for accuracy and transferability.[S4] The pseudopotentials were employed in conjunction with plane waves up to a kinetic energy cutoff of 630 eV. The calculations were carried out with the PBE exchange-correlation functional.[S5] Monkhorst-Pack grids[S6] were used for Brillouin zone integrations with a distance of < 0.025 Å^{-1} between grid points. A dispersion correction according to Grimme *et al.* was used.[S7] Convergence criteria included an energy change of $< 5\times10^{-6}$ eV/atom, a maximal force of < 0.008 eV/Å, and a maximal deviation of the stress tensor < 0.02 GPa from the imposed stress tensor. Optical properties were computed as described by Refson *et al.*[S8] Phonon frequencies were obtained from density functional perturbation theory (DFPT) calculations. Raman intensities and NLO properties were computed using DFPT with the '2n+1' theorem approach.[S9] It should be stressed that all calculations were carried out in the athermal limit, i.e., the influence of temperature and zero-point motion were not taken into account.

Band structure calculations resulted in a band gap of 2.9 eV. However, the apparent agreement with the experimentally determined optical band gap of 2.8 eV (*see main paper: Figure 5*) is somewhat fortuitous as DFT-GGA-PBE calculations are known to underestimate the band gap systematically. The top-most valence bands and the lower-most conduction bands are nearly dispersionless.

References

S1 C. E. Mortimer and U. Müller, Chemie - *Das Basiswissen der Chemie.* Thieme, Stuttgart 2003.

S2 P. Hohenberg and W. Kohn, *Phys. Rev. B*, 1964, **136**, 864-871.

S3 S. J. Clark, M. D. Segall, C. J. Pickard, P. J. Hasnip, M. J. Probert, K. Refson and M. C. Payne, *Z. Kristallogr.*, 2005, **220**, 567-570.

S4 J. P. Perdew, K. Burke and M. Ernzerhof, *Phys. Rev. Lett.*, 1996, **77**, 3865-3868.

S5 K. Lejaeghere, G. Bihlmayer, T. Björkman, P. Blaha, S. Blügel, V. Blum, D. Caliste, et al. *Science*, 2016, **351**, aad3000-1-aad3000-7.

S6 H. J. Monkhorst and J. D. Pack, *Phys. Rev. B*, 1976, **13**, 5188-5192.

S7 S. Grimme, J. Antony, S. Ehrlich and H. Krieg, *J. Chem. Phys.*, 2010, **132**, 154104(1-19).

S8 K. Refson, P. R. Tulip and S. J. Clark, *Phys. Rev. B*, 2006, **73**, 155114(1-12).

S9 K. Miwa, *Phys. Rev. B*, 2011, **84**, 094304(1-13).